

# UC San Diego

## UC San Diego Previously Published Works

### Title

QUANTITATIVE ANALYSIS OF THE INNER RETINAL LAYER THICKNESSES IN AGE-RELATED MACULAR DEGENERATION USING CORRECTED OPTICAL COHERENCE TOMOGRAPHY SEGMENTATION

### Permalink

<https://escholarship.org/uc/item/6sn103j9>

### Journal

Retina, 38(8)

### ISSN

0275-004X

### Authors

Muftuoglu, Ilkay Kilic  
Ramkumar, Hema L  
Bartsch, Dirk-Uwe  
et al.

### Publication Date

2018-08-01

### DOI

10.1097/iae.0000000000001759

Peer reviewed



Published in final edited form as:

Retina. 2018 August ; 38(8): 1478–1484. doi:10.1097/IAE.0000000000001759.

## QUANTATIVE ANALYSIS OF THE INNER RETINAL LAYER THICKNESSES IN AGE-RELATED MACULAR DEGENERATION USING CORRECTED OPTICAL COHERENCE TOMOGRAPHY SEGMENTATION

Ilkay Kilic Muftuoglu, MD<sup>1,2</sup>, Hema L. Ramkumar, MD<sup>1</sup>, Dirk-Uwe Bartsch, PhD<sup>1</sup>, Amit Meshi, M.D<sup>1</sup>, Raouf Gaber, M.D<sup>1</sup>, and William R. Freeman, MD<sup>1,\*</sup>

<sup>1</sup>Department of Ophthalmology, Jacobs Retina Center, Shiley Eye Institute, University of California San Diego, CA, US

<sup>2</sup>Also affiliated with Department of Ophthalmology, Istanbul Training and Research Hospital, Istanbul, Turkey

### Abstract

**Purpose**—To characterize inner retinal damage in dry age-related macular degeneration (AMD) patients using high resolution spectral-domain optical coherence tomography (SD-OCT) images.

**Methods**—Sixty eyes of 60 AMD patients were categorized using the Age-Related Eye Disease Severity (AREDS) severity scale. SD-OCT images of these patients were quantified by manually correcting the segmentation of each retinal layer, including the retina nerve fiber layer (RNFL), ganglion cell layer (GCL), and inner plexiform layer (IPL) to ensure accurate delineation of layers. The mean ganglion cell complex (GCC) thickness values (GCL+IPL+RNFL) were compared with 30 eyes of 30 healthy subjects.

**Results**—Ninety percent of eyes (81 eyes) required manual correction of segmentation. Compared to healthy subjects, mean GCC thicknesses significantly decreased in more advanced dry AMD eyes, and this decrease was predominantly related to a change in IPL thickness. There was no significant difference in thickness-related measurements between milder dry AMD (AREDS-2) eyes and healthy eyes ( $p>0.05$ ).

**Conclusion**—In patients with dry AMD, automatic OCT segmentation algorithms may be erroneous. As the severity of dry AMD increases, the IPL layer becomes thinned, suggesting that transsynaptic degeneration may be occurring as the photoreceptor layer is affected by AMD.

### Keywords

AMD; dry age-related macular degeneration; OCT; ganglion cell layer; GCC; ganglion cell complex; inner retinal layers; retinal layer segmentation

---

\*Corresponding author: William R. Freeman, MD, Address: University of California San Diego, Jacobs Retina Center, Shiley Eye Institute, 9415 Campus Point Drive, La Jolla, CA 92037, wrfreeman@ucsd.edu Phone: (858) 534-3513.

## INTRODUCTION

Age-related macular degeneration (AMD) is the leading cause of vision loss with an estimated prevalence of 6.5% among people 40 years of age and older in the United States.<sup>1</sup> Moreover, the number of people having AMD would be expected to increase by 50% to 2.95 million in 2020 due to a rapidly increasing aging population.<sup>1,2</sup>

Age-related macular degeneration is generally felt to be a disease of the outer retina, and tissue replacement therapy in eyes with AMD such as stem cell therapy, RPE transplantation, or retinal prostheses are being investigated.<sup>3,4,5</sup> It is important to know if replacing the RPE and/or photoreceptor layer can restore vision when there is a damage to the inner retina. For this reason, the ability to study inner retinal structures in eyes with AMD will give important information on the limits of therapy in patients with advanced outer retinal diseases.

Optical coherence tomography (OCT) has become the standard imaging modality to diagnose and guide treatment for various retinal diseases.<sup>6,7</sup> Recently introduced automated segmentation software enables *in vivo* quantitative and qualitative analyses of retinal layers.<sup>6</sup> The retinal ganglion cell complex (GCC), comprised of the retina nerve fiber layer (RNFL), ganglion cell layer (GCL), and inner plexiform layer (IPL), has been used as a diagnostic marker in glaucoma.<sup>8</sup> Recently, the automatic GCC algorithm has gained a popularity among retinal specialists, and GCC thicknesses have been studied in several diseases including diabetic retinopathy,<sup>9</sup> macular telangiectasia,<sup>10</sup> and AMD.<sup>11–15</sup> In diabetes mellitus, it has been shown that changes in GCC may occur before the development of clinically evident retinopathy. Similarly, studies evaluating the inner retinal changes in patients with dry AMD showed that the GCC significantly decreased even in the early stages of the AMD disease.<sup>11–15</sup> However, in all prior studies, the GCC was analyzed using automated segmentation without checking the accuracy of delineation of segmented retinal layers. Indeed, the OCT device used (Cirrus, Zeiss, Germany) does not allow manual correction of retinal layers and it has been also previously shown that automated segmentation can be affected by retinal atrophy or elevation.<sup>16</sup> Moreover, despite optimized software, segmentation errors occur in 26.8% scans and are more common than patient- or operated-related errors.<sup>17</sup> On the other hand, in the previous reports, no information has been provided on whether eyes with DM and high myopia were included, which may bias results. Thus, accurate delineation of retina layers with a refined study population is essential to better understand the disease pathogenesis. For these reasons, we wished to study the inner retinal layers in dry AMD patients with strict inclusion and exclusion criteria using high resolution SD-OCT images with accurate segmentation, and we compared our results with age-matched healthy subjects using the most recent high resolution Spectralis SD-OCT software.

## METHODS

This was a retrospective study of 60 dry AMD patients and 30 age-matched healthy controls. The University of California, San Diego Institutional Review Board approval was acquired for the review and analysis of patients medical records. The study adhered to the tenets of

the Declaration of Helsinki for research involving human subjects and complied with Health Insurance Portability and Accountability Act (HIPAA) regulations.

Patients with a diagnosis of dry AMD who were referred to the Jacobs Retina Center at the Shiley Eye Institute, Department of Ophthalmology, University of California, San Diego between 2008 and 2015 were selected using a search of a local database server. Then, multimodal imaging including spectral domain optical coherence tomography (SD-OCT), fluorescein angiography (FA), autofluorescence, and infrared reflectance using the Heidelberg Spectralis (Spectralis HRA-OCT; software 6i, Heidelberg Engineering, Carlsbad, California, USA) was reviewed. When 2 eyes of the same subject were eligible, one randomly selected eye of each subject was included. We hypothesized that the change in retinal layer thicknesses would not be the same in eyes with differing severity of dry AMD. Thus, we categorized the patients based on the Age Related Eye Disease Study (AREDS) classification into AREDS-2 or AREDS-3 to show the change in individual retinal thickness layers in different severity of the disease using multimodal imaging. We are aware that this classification might be ordinal in an era of advanced imaging instruments. However, this has been used in clinical trials and would give an opportunity to compare our results with previously reported studies. Based on this classification, category 2 was defined as the presence of multiple small drusen, and category 3 was defined as the presence of numerous medium drusen or one or more large drusen ( $>125\ \mu\text{m}$ ). All imaging modalities were reviewed by two independent retina specialists (I.K.M. and R.G.) at different sessions to ensure grading accuracy. When there was a disagreement, the decision of a third experienced physician's decision (W.R.F.) was asked, and a consensus was achieved for all cases.

### OCT Image Acquisition and Evaluation of Retinal Layers

All scans were acquired after optimal pupil dilation using the most recent Spectralis OCT Heidelberg Eye Explorer mapping software (version 6.0c). Macula volume cubes centered on the fovea consisting of at least 49 B-scans with a minimum of 9 automated real time-repetition rate (ART) were obtained. The inbuilt software defined the RNFL, GCL, and IPL thicknesses as the distance between internal limiting membrane (ILM) and outer boundary of RNFL, the distance between outer boundary of RNFL and outer boundary of ganglion layers, and the distance between the outer boundary of ganglion cells and outer boundary of inner plexiform layer, respectively.

In each case, the auto-segmentation mode automatically defined the inner and outer boundary of retinal layers was first activated. Then, all scans were carefully checked for the segmentation errors. Segmentation error was defined as improper delineation of the presentative lines in any portion of at least one cross-sectional images.<sup>19</sup> The need for accurate delineation was noted. If needed, manual adjustment was done starting from the innermost layer towards the outer retinal layers paying close attention to the reflectivity of each layer. When the software was not able to draw the borders of each layer, boundary lines were manually drawn using the software's caliper function. If the outer and/ or inner boundary deviated away from the exact location at another level, careful manual adjustment was done. As a last step, RNFL, GCL, and IPL thicknesses were noted in macular subfields that were determined by the ETDRS circle with an inner (1 mm diameter) and outer circle (3

mm diameter) as follows: central (within 1 mm), superior, temporal, inferior and nasal quadrants. The total average thicknesses of parafoveal retinal layers were also reported. Central macular thickness (the average thickness within the 1 mm of ETDRS circle) was measured from the innermost ILM to Bruch-membrane complex with manual adjustment for all cases, paying close attention to cases with retina pigment epithelium-Bruch's membrane complex abnormalities. All images were analyzed by 2 independent experienced retina specialists (I.K.M. and R.G.) using the same computer display and monitor settings 24 hour apart.

Baseline demographic data including age, gender, and presence of systemic diseases were documented as recorded from the charts. A Snellen visual acuity (VA) and intraocular pressure (IOP) by Goldman applanation tonometry were obtained within one week of retinal image acquisition and recorded. Patients were also checked for the presence of refractive errors. An age-matched control group was selected from healthy subjects.

Exclusion criteria included history of glaucoma, intraocular hypertension, optic nerve disease, presence of refractive errors (spherical equivalent ranging from +3 D to -3 D), presence of vitreoretinal interface disorders, history of prior vitrectomy, history of any laser treatment, or any other retinal diseases likely affect to retinal layer thickness. Patients with a diagnosis of diabetes mellitus were also excluded due to potential confounding effect on the ganglion cell layer thickness.<sup>9</sup>

### Statistical Analysis

The agreement between the two graders was checked using the intraclass coefficient (ICC). In randomly selected images, the agreement for the mean RNFL, GGL, and IPL was found to be high (ICC=0.87, ICC=0.89, and ICC=0.87) among the observers. Continuous variables were reported as mean and standard deviation. Categorical variables were compared using the chi-squared test. Normality was checked using Kolmogorov-Smirnov test. One-way analysis of variance (ANOVA) with the Tukey test was used to compare mean outcomes in the three groups. The statistical significance level was set as  $p < 0.017$  for the Bonferroni correction comparing three different groups. All statistical analyses were done using SPSS (SPSS, Inc, Chicago, US) version 23.

## RESULTS

Sixty eyes of 60 patients with dry AMD and 30 eyes of 30 healthy subjects were included. In the overall study population, 90% of eyes (81 eyes) required manual correction in delineation of retinal layers in at least one B-scan. Four AREDS-3 eyes, three AREDS-2 eyes, and two eyes from the control subjects did not require manual correction of segmentation. The baseline characteristics of the patients are summarized in Table 1. There was no significant difference in IOP, spherical equivalent, or signal strength between groups. The BCVA was significantly lower in the AREDS-3 group compared to the control and AREDS-2 groups ( $p < 0.001$ ). In the overall study population, visual acuity (logMAR) was negatively correlated with mean GCL thickness ( $r = -0.26$ ,  $p = 0.015$ ), mean IPL thickness ( $r = -0.34$ ,  $p = 0.001$ ), and mean GCC thickness ( $r = -0.298$ ,  $p = 0.006$ ).

The AREDS-3 group had a significantly lower IPL thickness in all parafoveal quadrants ( $p < 0.05$ ), except the superior quadrant and the central  $1 \text{ mm}^2$  when compared to healthy eyes ( $p = 0.07$ ,  $p = 0.37$  respectively). The mean decrease in IPL thickness in the AREDS-3 group was very mild, 1.9% in the central  $1 \text{ mm}^2$ , and 6.8% in the central  $3 \text{ mm}^2$  when compared to the control group. Moreover, the decrease in mean IPL thickness was most prominent in temporal quadrant (8.5%), followed by the nasal (8.1%), inferior (7.2%), and superior (5.8%) quadrants. Table 2 shows the distribution of mean RNFL, GCL, and IPL thicknesses among dry AMD patients and control subjects.

Though mean GCL thickness was slightly thinner in all quadrants in the AREDS-3 group compared to the AREDS-2 group and healthy subjects, there was no significant difference in mean GCL thickness in any quadrant in the three groups ( $p > 0.05$  for all comparisons).

The mean GCC thickness in the temporal and inferior quadrants were significantly lower in AREDS-3 group compared to the control group ( $p < 0.05$ ). However, there was no significant difference in the mean GCC thickness in the central  $1 \text{ mm}$  of the ETRDS circle, superior and nasal quadrants between the groups. The decrease in GCC thickness was mostly due to the thinner IPL layer in the AREDS-3 group. Figure 1 shows the distribution of GCC thickness in different quadrants among the groups. There was a mild decrease in mean GCC thickness within central  $1 \text{ mm}^2$  (less than 1.0%). The most prominent decrease in mean GCC thickness was detected in inferior (6.5%) quadrant followed by temporal (5.8%) and nasal quadrant (5.3%). The average total decrease in GCC within the central  $3 \text{ mm}^2$  was 4.5% in AREDS-3 group compared to control subjects.

Despite significant differences in some inner retinal layers between the control and AREDS-3 group, the AREDS-2 group did not exhibit any difference in inner retinal layer thicknesses.

The mean RNFL thickness in all quadrants was similar in the three groups ( $p > 0.05$  for all quadrants, one-way ANOVA). Additionally, there was no significant difference in CMT among the 3 groups ( $p > 0.05$ , one-way ANOVA).

## DISCUSSION

In this study, after manual correction of segmentation to ensure appropriate delineation in the majority of patients, we show that the RNFL and GCL are preserved in the central fovea and parafovea in dry AMD patients. However, as disease progresses in dry AMD patients, the inner plexiform layer becomes involved. A decrease in mean IPL thickness is seen most prominently in horizontal quadrants with the least decrease in the central fovea, and a decrease in GCC thickness is present in the inferior quadrant followed by the temporal quadrant. Since the GCL is absent over the fovea, these findings may suggest that trans-synaptic degeneration occurs first with dendrite loss, and the parafovea is more vulnerable to inner retinal changes in dry AMD. Another hypothesis may be that the retinal photoreceptors as well as cells in the inner retinal layers, particularly inner nuclear layer, are chronically hypoperfused and ischemic from microvascular choroidal damage from AMD.<sup>20</sup>

In accordance with our results, a histopathologic study comparing the number of ganglion cell layer neurons in eyes with dry AMD and controls found that the number of ganglion cells were similar in all groups. Moreover, investigators demonstrated that the number of the macular photoreceptors in dry AMD patients was similar to the number in control eyes with a moderate loss in the parafovea.<sup>12</sup>

Despite a significant increase in the recently published reports assessing the GCC change in various disease including AMD,<sup>11-14</sup> we are not aware of any study evaluating the GCC using accurate manually corrected retinal segmentation. In all previous cross-sectional reports analyzing the morphologic changes in the inner retina in AMD patients, automated segmentation obtained by Cirrus OCT was used.<sup>11-14</sup> However, the latest commercial retinal layer segmentation algorithm on the Cirrus OCT has scan artifacts and errors in the ganglion cell algorithm in healthy eyes as often as 26.8%. Among the scans with errors, segmentation errors are more common than operator-related errors, which would likely introduce bias including over or underestimation of inner retinal layers. It is also likely that these errors are more frequent in the presence of retinal diseases.<sup>16</sup> In order to minimize software-related issues, we carefully checked all scans to ensure accurate delineation of each inner retinal layer. Though the rate and causes of software algorithm errors were not the main outcome of our study, we noted that almost 90% of eyes required manual correction of segmentation, suggesting that interpretation of results without manual correction and/ or lack of confirmation of accurate segmentation may be very misleading.

Table 3 shows the difference in the method and results between prior published reports and our study; however due to the difference in imaging algorithms and instruments used (Spectralis versus Cirrus OCT), this comparison is not a head to head comparison. The Cirrus OCT measures the ganglion cell-inner plexiform layer thickness automatically using 3-dimensional information from the macular cube in an oval annulus shape. The annulus comprises a vertical inner and outer diameter of 1.2 and 4.8 mm, respectively. However, using Spectralis we reported the thickness-related parameters based on ETDRS circle in the central subfield area (1 mm of fovea) and parafovea (3 mm of fovea).

There are some limitations of our study, including a relatively small cohort of patients and cross-sectional study design. We did not include those with advanced geographic atrophy, however a study showing the change in ganglion cell layer thickness has been submitted for publication by our group. We are also aware of studying retinal thickness in several quadrants, which would likely introduce type 1-error in the statistics, however we believe that only further studies with a very large number of patients would eliminate this bias. Despite these limitations, to the best of our knowledge, this is the first study assessing the ganglion cell complex in dry and wet AMD patients using appropriate segmentation of retinal layers. We inspected at least 49 B-scan images per eye to overcome the software-related segmentation errors and believe that a well-defined study population with strict exclusion criteria allows us to draw reliable conclusions from the results.

In conclusion, in mild and intermediate dry AMD patients, inner retinal layers including retina nerve fiber layer and ganglion cell layers are well-preserved in the central fovea and parafovea despite some disruption in outer retinal layers, consistent with histopathologic

reports. However, as macular degeneration progress, the inner plexiform layer becomes thinned, suggesting that trans-synaptic degeneration of ganglion cell dendrites occurs with photoreceptor loss. The total average decrease in GCC within 3 mm<sup>2</sup> was modest, 4.5%, and this decrease was mostly prominent in the inferior quadrant followed by temporal quadrant. This finding suggests that there may be still more than adequate inner retinal cellular density to permit the goal of high resolution retinal prosthesis or transplantation of photoreceptor or RPE complex to salvage vision in AMD eyes.

## Acknowledgments

**Financial Support:** Supported in part by NIH grant R01 EY016323-09A1 (D.U.B.), a core grant from the National Eye Institute P30 EY022589 (WRF) and an unrestricted grant from Research to Prevent Blindness, NY (WRF). The funding organizations had no role in the design or conduct of this research.

## References

- 1 Klein R, Chou CF, Klein B, et al. Prevalence of Age-Related Macular Degeneration in the US Population. *Arch Ophthalmol*. 2011; 129:75–80. [PubMed: 21220632]
- 2 Wong WL, Su X, Li X, et al. Global prevalence of age-related macular degeneration and disease burden projection for 2020 and 2040: a systematic review and meta-analysis. *Lancet Glob Health*. 2014; 2:106–116.
- 3 Schwartz SD, Tan G, Hosseini H, Nagiel A. Subretinal Transplantation of Embryonic Stem Cell-Derived Retinal Pigment Epithelium for the Treatment of Macular Degeneration: An Assessment at 4 Years. *Invest Ophthalmol Vis Sci*. 2016; 57:ORSFc1–9. [PubMed: 27116660]
- 4 Eng JG, Agrawal RN, Tozer KR, et al. Morphometric analysis of optic nerves and retina from an end-stage retinitis pigmentosa patient with an implanted active epiretinal array. *Invest Ophthalmol Vis Sci*. 2011; 52:4610–4616. [PubMed: 21296811]
- 5 Choudhary P, Gutteridge A, Impney E, et al. Targeting the cAMP and Transforming Growth Factor- $\beta$  Pathway Increases Proliferation to Promote Re-Epithelialization of Human Stem Cell-Derived Retinal Pigment Epithelium. *Stem Cells Transl Med*. 2016; 5:925–937. [PubMed: 27112176]
- 6 Barteselli G, Bartsch DU, Weinreb RN, et al. Real-time full-depth visualization of posterior ocular structures: Comparison Between Full-Depth Imaging Spectral Domain Optical Coherence Tomography and Swept-Source Optical Coherence Tomography. *Retina*. 2016; 36:1153–1161. [PubMed: 26562563]
- 7 Barteselli G, Bartsch DU, Viola F, et al. Accuracy of the Heidelberg Spectralis in the alignment between near-infrared image and tomographic scan in a model eye: a multicenter study. *Am J Ophthalmol*. 2013; 156:588–92. [PubMed: 23769196]
- 8 Kim HJ, Lee SY, Park KH, et al. Glaucoma Diagnostic Ability of Layer-by-Layer Segmented Ganglion Cell Complex by Spectral-Domain Optical Coherence Tomography. *Invest Ophthalmol Vis Sci*. 2016; 1:57:4799–4805.
- 9 Chhablani J, Sharma A, Goud A, et al. Neurodegeneration in Type 2 Diabetes: Evidence From Spectral-Domain Optical Coherence Tomography. *Invest Ophthalmol Vis Sci*. 2015; 56:6333–6338. [PubMed: 26436886]
- 10 Chhablani J, Rao HB, Begum VU, et al. Retinal ganglion cells thinning in eyes with nonproliferative idiopathic macular telangiectasia type 2A. *Invest Ophthalmol Vis Sci*. 2015; 56:1416–1422. [PubMed: 25655800]
- 11 Zucchiatti I, Parodi MB, Pierro L, et al. Macular ganglion cell complex and retinal nerve fiber layer comparison in different stages of age-related macular degeneration. *Am J Ophthalmol*. 2015; 160:602–607. [PubMed: 26052088]
- 12 Lee EK, Yu HG. Ganglion Cell-Inner Plexiform Layer and Peripapillary Retinal Nerve Fiber Layer Thicknesses in Age-Related Macular Degeneration. *Invest Ophthalmol Vis Sci*. 2015; 56:3976–3983. [PubMed: 26087362]

- 13 Savastano MC, Minnella AM, Tamburrino A, et al. Differential vulnerability of retinal layers to early age-related macular degeneration: evidence by SD-OCT segmentation analysis. *Invest Ophthalmol Vis Sci.* 2014; 29:560–566.
- 14 Yenice E, engün A, Soyugelen Demirok G, Turaçlı E. Ganglion cell complex thickness in nonexudative age-related macular degeneration. *Eye (Lond).* 2015; 29:1076–1080. [PubMed: 26021868]
- 15 Medeiros NE, Curcio CA. Preservation of ganglion cell layer neurons in age-related macular degeneration. *Invest Ophthalmol Vis Sci.* 2001; 42:795–803. [PubMed: 11222543]
- 16 Lee HJ, Kim MS, Jo YJ, Kim JY. Ganglion Cell-Inner Plexiform Layer Thickness in Retinal Diseases: Repeatability Study of Spectral-Domain Optical Coherence Tomography. *Am J Ophthalmol.* 2015; 160:283–289. [PubMed: 26004405]
- 17 Alshareef RA, Dumpala S, Rapole S, et al. Prevalence and Distribution of Segmentation Errors in Macular Ganglion Cell Analysis of Healthy Eyes Using Cirrus HD-OCT. *PLoS One.* 2016; 18:e0155319.
- 18 The Age-Related Eye Disease Study Severity Scale for Age-Related Macular Degeneration AREDS Report No. 17. *Arch Ophthalmol.* 2005; 123:1484–1498. [PubMed: 16286610]
- 19 Hwang YH, Kim MK, Kim DW. Segmentation Errors in Macular Ganglion Cell Analysis as Determined by Optical Coherence Tomography. *Ophthalmology.* 2016; 123:950–958. [PubMed: 26854040]
- 20 Saha S, Greferath U, Vessey KA, et al. Changes in ganglion cells during retinal degeneration. *Neuroscience.* 2016; 329:1–11. [PubMed: 27132232]

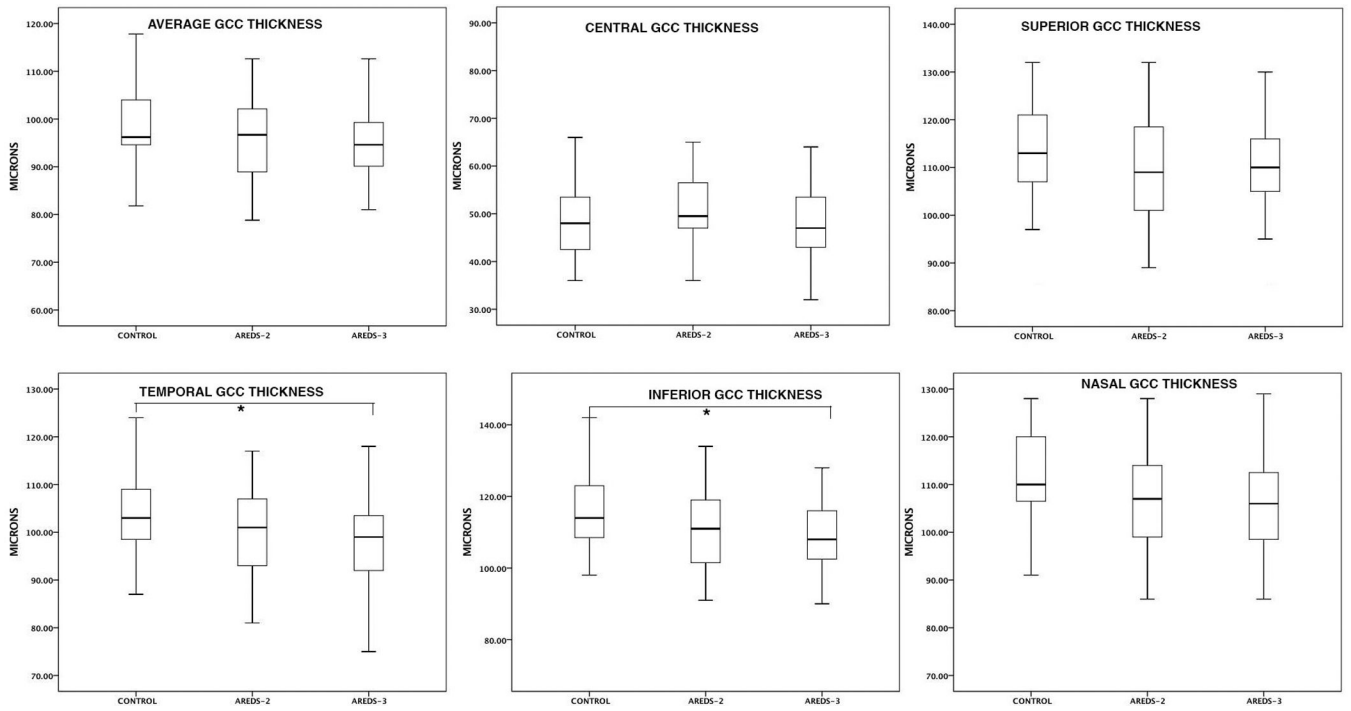


**Figure 1.** The distribution of ganglion cell complex thicknesses in different quadrants among the study population. \*refers statistically significant p value between the control group and AREDS-3 group.

**Table 1**

Baseline demographics of the study population

|  | <b>CONTROL-<br/>GROUP</b> | <b>AREDS-2<br/>GROUP</b> | <b>AREDS-3<br/>GROUP</b> | <b>P</b> |
|--|---------------------------|--------------------------|--------------------------|----------|
| <b>Number of patients</b>                | 30                        | 30                       | 30                       |          |
| <b>Mean age Standard deviation, year</b> | 74.1±9.8                  | 74±12                    | 73.5±11                  | 0.78 *   |
| <b>Gender, female (n)</b>                | 15                        | 15                       | 15                       |          |
| <b>Spherical Equivalent, Diopter</b>     | -0.25±1.6                 | -0.1±1.6                 | 0.56±1.3                 | 0.32 *   |
| <b>Intraocular pressure, mean (mmHg)</b> | 14.5±3.1                  | 14.8±3.1                 | 14.6±3.3                 | 0.67 *   |
| <b>BCVA, logMAR</b>                      | 0                         | 0.10±0.02                | 0.17±0.02                | <0.001 * |
| <b>Snellen Equivalent</b>                | 20/20                     | ≈20/25                   | ≈20/30                   |          |
| <b>Signal Strength</b>                   | 66±4.3                    | 66±7.6                   | 66±4.5                   | 0.83 *   |

BCVA=best-corrected visual acuity

\* one-way ANOVA

Parameters are presented as mean and standard deviation

**Table 2**

Distribution of the inner retinal layer thicknesses in the study population

|                            | Control Group | AREDS-2  | AREDS-3   | P*           |
|----------------------------|---------------|----------|-----------|--------------|
| <b>Mean RNFL thickness</b> |               |          |           |              |
| Central 1mm <sup>2</sup>   | 12.8±1.8      | 13.5±2.1 | 12.6±2.3  | 0.60         |
| Superior                   | 23.1±1.1      | 24.0±3.2 | 24.6±3.5  | 0.12         |
| Temporal                   | 17.8±1.5      | 17.6±1.5 | 18.2±2.0  | 0.55         |
| Inferior                   | 25.0±2.7      | 25.0±2.8 | 23.7±3.4  | 0.23         |
| Nasal                      | 20.4±2.3      | 20.5±2.5 | 20.9±2.2  | 0.62         |
| Total Average              | 19.8±0.2      | 20.1±0.3 | 20.0±0.34 | 0.85         |
| <b>Mean GGL thickness</b>  |               |          |           |              |
| Central 1mm <sup>2</sup>   | 14.7±2.8      | 15.8±3.4 | 15±3.1    | 0.52         |
| Superior                   | 50.4±5.4      | 48.4±5.3 | 48.1±4.8  | 0.17         |
| Temporal                   | 44.7±5.3      | 43.5±5.4 | 42.7±5.2  | 0.15         |
| Inferior                   | 50.6±5        | 48.4±5.1 | 48.2±5.9  | 0.04         |
| Nasal                      | 49.3±5.8      | 48.5±5.7 | 47.2±7.6  | 0.10         |
| Total Average              | 41.9±0.8      | 40.9±0.8 | 40.2±0.8  | 0.14         |
| <b>Mean IPL thickness</b>  |               |          |           |              |
| Central-1mm <sup>2</sup>   | 20.9±2.9      | 21.8±3.2 | 20.5±3.4  | 0.37         |
| Superior                   | 39.7±3.9      | 38.1±4.6 | 37.4±3.2  | 0.07         |
| Temporal                   | 40.9±3.3      | 39.3±4   | 37.6±3.7  | <b>0.003</b> |
| Inferior                   | 40.2±3.1      | 38.3±4   | 37.3±3.5  | <b>0.010</b> |
| Nasal                      | 41.8±3.4      | 39.8±4.3 | 38.6±4.1  | <b>0.009</b> |
| Total average              | 36.7±0.5      | 35.5±0.7 | 34.3±0.5  | 0.02         |

RNFL=retina nerve fiber layer, GCL=ganglion cell layer, IPL=inner plexiform layer, superior=

Total average=mean thickness within 3 mm of Early Treatment Diabetic Retinopathy Study circle

Variables are represented in microns as mean ±standard deviation, p= p value,

\* one-way ANOVA

Note, there is no significant difference in any retina layer thickness between control subjects and AREDS-2 group.

**Table 3**  
Comparison of groups evaluating ganglion cell complex in dry age-related macular degeneration

| Group                             | Study population                         | OCT device | GCC segmentation algorithm                         | Change in GCC   | Isolated GCC layers | Exclusion of high myopia/ presence of DM  |
|-----------------------------------|--|------------|--|---|---------------------|---|
| Zucchiatti et al. <sup>8</sup>    | Dry AMD subgroups as AREDS-2, AREDS-3    | Cirrus     | Automated  | <ul style="list-style-type: none"> <li>- Decrease in mean GCC thickness in AREDS-2 and AREDS-3 (borderline)</li> <li>- No information on quadrants</li> </ul> | (-)                 | Information not provided  |
| Savastano MC et al. <sup>10</sup> | Early AMD (no exact definition)          | n/a        | Customized automated segmentation                  | <ul style="list-style-type: none"> <li>- Decrease</li> <li>- No info on quadrants</li> </ul>  | (-)                 | Information not provided  |
| Yenice et al. <sup>11</sup>       | Dry AMD (no subgroups)                   | Cirrus     | Automated  | Decrease in GCC in all quadrants  | (-)                 | Information not provided  |
| Lee EK et al. <sup>9</sup>        | Dry AMD (AREDS-3)                        | Cirrus     | Automated Segmentation failures excluded           | <ul style="list-style-type: none"> <li>- Decrease in mean GCC at all sectors</li> </ul>   | (-)                 | <ul style="list-style-type: none"> <li>- High myopia excluded</li> <li>- Information not provided for DM</li> </ul> |
| Muftuoglu et al.                  | Dry AMD subgroups as AREDS-2 and AREDS-3 | Spectralis | Automated software with accurate manual correction | Decrease  | (+)                 | Excluded  |

OCT=optical coherence tomography, AMD=age related macular degeneration, AREDS=age-related eye disease study, GCC=ganglion cell complex, DM=diabetes mellitus